

Chemical Design of ^{99m}Tc -Labeled Probes for Targeting Osteogenic Bone Region

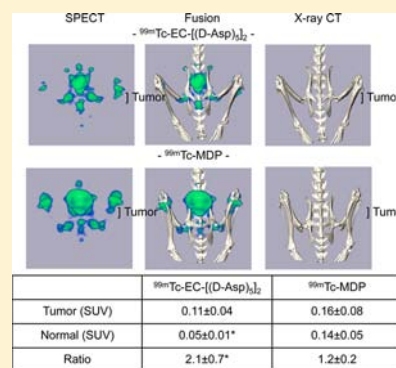
Mashiho Yanagi,[†] Tomoya Uehara,^{*,†} Yukie Uchida,[†] Sachiko Kiyota,[†] Mai Kinoshita,[†] Yusuke Higaki,[†] Hiromichi Akizawa,[‡] Hirofumi Hanaoka,[†] and Yasushi Arano[†]

[†]Graduate School of Pharmaceutical Sciences, Chiba University, 1-8-1 Inohana, Chuo-ku, Chiba, 263-8675, Japan

[‡]Showa Pharmaceutical University, 3-3165 Higashi-Tamagawagakuen, Machidashi, Tokyo, 194-8543, Japan

S Supporting Information

ABSTRACT: Radionuclide bone imaging using polynuclear ^{99m}Tc complexes of bisphosphonates is the most common clinical practice in nuclear medicine. However, the improvement in the contrast between normal and osteogenic bone regions has been required. Herein we reported a new ^{99m}Tc -labeled compound considering the increased vascular permeability of osteogenic region. We selected penta-D-Asp as both a targeting motif to hydroxyapatite (HA) and a molecular size modifier, and two penta-D-Asp molecules were conjugated with the two carboxylate residues of ethylene dicysteine (EC) selected as the ^{99m}Tc chelating moiety to prepare EC-[(D-Asp)₅]₂. The molecular size, HA binding, and pharmacokinetics of ^{99m}Tc -EC-[(D-Asp)₅]₂ in normal mice and model rats bearing osteogenic tumor were compared to those of ^{99m}Tc -MDP and ^{99m}Tc -EC with one (D-Asp)₅ motif, ^{99m}Tc -EC-(D-Asp)₅. The molecular size of ^{99m}Tc -EC-[(D-Asp)₅]₂ was higher than that of ^{99m}Tc -MDP and ^{99m}Tc -EC-(D-Asp)₅ when determined by permeability of the ^{99m}Tc -compounds through a membrane filter (10 kDa). The HA binding of ^{99m}Tc -EC-[(D-Asp)₅]₂ was higher than and similar to that of ^{99m}Tc -EC-(D-Asp)₅ and ^{99m}Tc -MDP. ^{99m}Tc -EC-[(D-Asp)₅]₂ exhibited significantly lower accumulation in normal bone of mice than did ^{99m}Tc -MDP. In osteogenic tumor bearing model rats, ^{99m}Tc -EC-[(D-Asp)₅]₂ accumulated in the osteogenic and normal bone region similar to and lower than ^{99m}Tc -MDP, respectively. Although further studies including the chain length of D-Asp are required, these findings indicated that the present chemical design of ^{99m}Tc -labeled probe would be applicable to develop ^{99m}Tc -labeled probes for selective imaging of osteogenic bone region as well as develop therapeutic agents using therapeutic radionuclides such as ^{90}Y , ^{177}Lu , ^{186}Re , or ^{188}Re and cytotoxic agents to osteogenic bone tumor region.



■ INTRODUCTION

Radionuclide bone imaging using technetium-99m-methylenediphosphonate (^{99m}Tc -MDP) and ^{99m}Tc -hydroxymethylenediphosphonate (^{99m}Tc -HMDP) is the most common clinical practice in nuclear medicine over 40 years.^{1–4} In ^{99m}Tc -MDP and ^{99m}Tc -HMDP, MDP, or HMDP acts as both a bone-targeting device and a coordinating ligand for ^{99m}Tc to form polynuclear ^{99m}Tc complexes. However, they are not single, well-defined chemical species, but mixtures of short- and long-chain polymers in which one or more technetium atoms are bridged by two or several phosphate and hydroxyl groups. Different polymers can have a different degree of ionization and biological behavior.^{5,6} An interval of 2–6 h is needed between injection and bone imaging because of their slow clearance from soft tissues.^{7,8} Shortening this interval would lessen the burden on patients in terms of the total length of examination and the dose of radiation absorbed.

To circumvent the problems associated with ^{99m}Tc -MDP and ^{99m}Tc -HMDP, a new class of ^{99m}Tc -labeled bisphosphonate was developed. In this design, an amine group tethered from the carbon atom of a bisphosphonate was conjugated with a carboxylate of a mononuclear ^{99m}Tc complex of high in vivo

stability so that the inherent bisphosphonate structure remains intact.^{9–16} They exhibited rapid clearance from blood and accumulated well in the bone, due to their strong hydroxyapatite (HA) binding ability. However, they suffered from low contrast between normal bone and osteogenic bone tumor regions, since they do not differentiate the two bone regions. These results call for another class of radiolabeled probes that possess selectivity in osteogenic bone tumor region.

It is well-known that angiogenesis is essential not only for tumor growth but also for bone repair and development.^{17,18} The microvessels of normal bone form a regular vascular network with a tissue-specific structure, branching pattern, and size-range. They are distributed at regular and closely spaced intervals. The vessels in bone tumor, on the other hand, differ markedly from the normal vascular architecture in their organization, structure, and function. They exhibit a serpentine course, branch irregularly, and form arterio-venous shunts.¹⁹ The permeability of tumor vessels is in general higher than that

Received: April 18, 2013

Revised: June 4, 2013

Published: June 12, 2013

of normal vessels.¹⁸ These studies suggested that selective targeting to osteogenic tumor region could be achieved with radiolabeled probes of high HA binding and appropriate molecular sizes.

Previous studies also indicated that repetitive acidic amino acid sequence such as oligo-aspartic acids (oligo-Asp) constitutes a HA binding motif.^{20,21} The binding affinities of oligo-Asps to HA depend only on the number of Asp residues, not on their optical characters, and the affinities increase with an increase in peptide chain length.²² The peptide consisting of L-Asp was rapidly degraded to shorter peptides in plasma, whereas the peptide of D-Asp was hardly degraded in plasma.²² In addition, our prior study of dendrimer derivatives suggested that the repetitive sequence of D-Asp would become an expanded form at neutral pH, due to the repulsion of each carboxylic acid, which would increase molecular size of the whole molecule.²³

Based on these studies and consideration, we selected penta-D-Asp as a targeting motif to HA and a molecular size modifier, and one or two penta-D-Asp molecules were conjugated with ethylene dicysteine (EC) selected as the ^{99m}Tc chelating moiety to prepare EC-(D-Asp)₅ or EC-[(D-Asp)₅]₂ (Figure 1). To

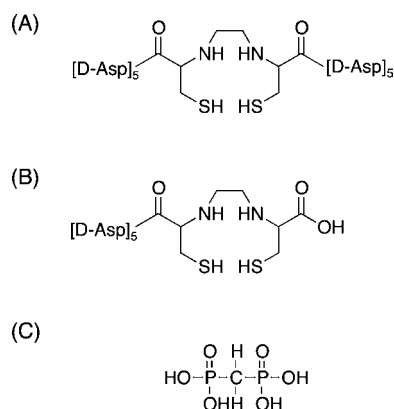


Figure 1. Structures of EC-[(D-Asp)₅]₂ (A), EC-(D-Asp)₅ (B), and MDP (C).

evaluate the present chemical design, the molecular size, HA binding, and pharmacokinetics in normal mice and rats bearing osteogenic tumor of the ^{99m}Tc-labeled compounds were compared in normal mice. The bone accumulation of ^{99m}Tc-EC-[(D-Asp)₅]₂ and ^{99m}Tc-MDP were also compared in rats bearing osteogenic tumor.

EXPERIMENTAL SECTION

Materials. ^{99m}Tc-Pertechnetate (^{99m}TcO₄⁻) was eluted in saline solution on a daily basis from Fujifilm RI Pharma Co., Ltd. generator (Chiba, Japan). Preparative reversed phase HPLC (Preparative RP-HPLC) was performed with a Cosmosil SC₁₈-AR-300 column (20 × 150 mm, Nacalai Tesque, Kyoto, Japan) connected to a Cosmosil SC₁₈-AR-300 guard column (10 × 20 mm, Nacalai Tesque) at a flow rate of 5 mL/min with 90% A (0.1% aqueous trifluoroacetic acid (TFA)) and 10% B (acetonitrile with 0.1% TFA) for the first 2 min, followed by a linear gradient of 90% A and 10% B to 80% A and 20% B in 60 min. The eluent was monitored at 220 nm with an ultraviolet (UV) detector. Analytical RP-HPLC was performed with a Cosmosil SC₁₈-AR-300 column (4.6 × 150 mm, Nacalai Tesque) at a flow rate of 1 mL/min with a gradient mobile

phase starting from 100% C (12.5 mM aqueous phosphoric acid) and 0% D (methanol) to 0% C and 100% D in 30 min. The eluent was monitored at 254 nm with an UV detector coupled to a NaI(Tl) radio-detector (Gabi star, Raytest, Strubenhardt, Germany). TLC analyses were performed with silica plates (Silica gel 60 F254, Merck, Tokyo) developed with chloroform. Paper chromatography (PC) analyses were performed with Whatman No. 1 (Whatman Japan Ltd., Tokyo) developed with saline. Fast-atom bombardment mass spectra (FAB-MS) were taken on a JEOL JMS-HX-110A mass spectrometer (JEOL Ltd., Tokyo). Matrix assisted laser desorption/ionization time-of-flight mass spectra (MALDI-TOF-MS) were taken on an AXIMA-CFR Plus (Shimadzu Ltd., Kyoto). Electrospray ionization mass spectra (ESI-MS) were taken on a MicroMS LCT Premier ToFMS spectrometer (Waters Japan, Tokyo). Proton nuclear magnetic resonance (¹H NMR) spectra were recorded on a JEOL JNM-ALPHA 400 spectrometer (JEOL Ltd.) with tetramethylsilane as an internal standard. Elemental analyses were performed by PE-2400 (Perkin-Elmer Japan, Tokyo). Two masses were reported for rhenium containing fragments to indicate the significant isotopic abundance of both ¹⁸⁵Re and ¹⁸⁷Re. Each peak was observed to have the proper relative abundance. Ethylene dicysteine (EC, **1**) was synthesized according to the procedure of Blondeau et al.²⁴ Other reagents were of reagent grade and used as received.

Preparation of (D-Asp)₅. (D-Asp)₅ was synthesized by manual Fmoc solid-phase method using *N*^α-Fmoc-D-Asp-(OtBu)-Alkoresin (250 mg, 0.15 mmol) as the solid phase. Side-chain protecting group was Asp(OtBu) (where tBu represents tert-butyl). The peptide chain was constructed manually according to the published method consisting of (I) 20 min of deprotection with 20% piperidine-dimethylformamide (piperidine-DMF, ca. 5 mL) and (II) 3 h of coupling of the Fmoc amino acid derivative (2.5 equiv) with 1-hydroxybenzotriazole (HOBt, 2.5 equiv) and 1,3-diisopropylcarbodiimide (DIPCI, 2.5 equiv) in DMF (5 mL).²⁵ Condensation reactions were continued until the resin became negative in the Kaiser test.²⁶ After assembling the respective amino acids, the *N*^α-Fmoc-[(D-Asp)(OtBu)]₅-resin was washed with dichloromethane (ca. 25 mL) and diethyl ether (ca. 25 mL).

Synthesis of S,S'-Bis-triphenylmethyl-ethylene Dicysteine (2). Compound **1** (4.45 g, 16.6 mmol) and triphenyl methanol (Trt-OH, 8.63 g, 33.2 mmol) was dissolved in TFA (119 mL) and mixed for 3 h. After the solvent was evaporated in vacuo, the residue was dissolved in diethyl ether (100 mL). The pH of the solution was adjusted to 3–5 with 10% aqueous CH₃COONa on ice. The precipitate was collected by suction filtration and washed with diethyl ether (300 mL). After the residue was suspended in hot methanol (300 mL), the remaining precipitate was removed by filtration. The filtrate was removed in vacuo, and compound **2** was obtained as a yellow solid (8.82 g, 70.7%). ¹H NMR (CD₃OD): δ 2.60 (4H, d, CH₂), 2.73 (2H, d, CH), 3.01 (4H, d, CH₂), 7.29 (30H, t, phenyl); FAB-MS (M+Na)⁺: *m/z* 775, Found: 775.

Synthesis of N,N'-Bis-*t*-butoxycarbonyl-S,S'-bis-triphenylmethyl-ethylene Dicysteine (3). Compound **2** (1.60 g, 2.12 mmol) was dissolved in a mixture of water and acetonitrile (1:1, 5.6 mL), and 1 N NaOH (4.24 mL) was added to the solution. After cooling to 0–5 °C, (Boc)₂O (2.04 g, 3.73 mmol) in acetonitrile (2.6 mL) was added, and the reaction mixture was stirred overnight at room temperature.

After the solution was acidified with 1% aqueous HCl, crude compound **3** was extracted with ethyl acetate (40 mL \times 3) and then dried over anhydrous CaSO₄. After removing the solvent in vacuo, the residue was purified with open column chromatography using silica gel and subsequent elution with chloroform:methanol (100:1) to produce compound **3** as a white solid (0.91 g, 44.8%). ¹H NMR (CDCl₃): δ 1.27 (18H, s, Boc), 2.12 (2H, d, CH), 2.63 (4H, d, CH₂), 3.23 (4H, dd, CH₂), 7.27 (30H, t, phenyl); FAB-MS (M+H)⁺: m/z 953, Found: 953.

Synthesis of EC-Conjugated Peptides (EC-[(D-Asp)₅]₂ (4a), EC-(D-Asp)₅ (4b). The N^α-Fmoc-[(D-Asp)(OtBu)]₅-resin (140 mg, 76.2 μ mol) was suspended in 20% piperidine-DMF (ca. 5 mL). After standing for 20 min, the [(D-Asp)(OtBu)]₅-resin was filtered off and washed with DMF (ca. 35 mL). The peptide(OtBu) resin (76.2 μ mol, 1.5 equiv), HOBt (15.2 mg, 99 μ mol, 2 equiv), DIPCI (15.5 μ L, 99 μ mol, 2 equiv), and EC(Boc)₂(Trt)₂ (48.6 mg, 51 μ mol, 1 equiv) were dissolved in DMF (ca. 2 mL) and mixed for 5 h. The EC(Boc)₂(Trt)₂-[(D-Asp)(OtBu)]₅-resin_n (n = 1 or 2) was filtered off and washed with DMF (ca. 5 mL). The EC(Boc)₂(Trt)₂-[(D-Asp)(OtBu)]₅-resin_n (n = 1 or 2) was then treated with a mixture of TFA (2.24 mL), water (0.14 mL), thioanisole (0.14 mL), *m*-cresol (0.07 mL), triisopropylsilane (0.07 mL), and 1,2-ethanedithiol (0.14 mL) for 2 h to remove the peptides from the resin and the protecting groups of amino acid simultaneously. The resin was removed by filtration, and the filtrate was treated with dry diethyl ether (ca. 5 mL) to precipitate the crude products. The precipitate was dissolved in water (5 mL) and washed with ether (5 mL \times 3). The solution was purified by preparative RP-HPLC, and the fractions containing the desired products were collected and lyophilized to afford compound **4a** (7.41%) and **4b** (18.7%). MALDI-TOF-MS: **4a** (M+H)⁺; m/z 1419, Found: 1419, **4b** (M+H)⁺; m/z 844, Found: 844.

Synthesis of Ethylene Dicycysteine Diethyl Ester (5). Compound **1** (1.0 g, 3.73 mmol) was suspended in ethanol (140 mL), which was saturated with dry HCl gas at -20°C . After the solution was refluxed for 5 h, the precipitate was removed by filtration. The filtrate was evaporated in vacuo, and the residue washed with ethanol (ca. 10 mL) to obtained compound **5** as a white solid (0.49 g, 40.6%). ¹H NMR [(CD₃)SO]: δ 1.31 (6H, t, CH₃), 3.06 (4H, m, CH₂), 4.49 (2H, t, CH), 3.44 (4H, t, CH₂), 4.26 (4H, m, CH₂); FAB-MS (M+H)⁺: m/z 325, Found: 325.

Synthesis of Ethylene Dicycysteine Diethyl Ester Oxorhenium(V) (6). This compound was synthesized according to the procedure of Green et al.²⁷ with slight modification as follows. Low-oxygen water (LOW) was prepared by purging Milli-Q water with N₂ gas. Compound **5** (250 mg, 0.63 mmol), ammonium perrhenate (169 mg, 6.30 mmol), and sodium hydrogen carbonate (106 mg, 1.26 mmol) were added to LOW (100 mL), and then the vial was sealed and the contents dissolved through sonication. The reaction vial solution was then purged with N₂ gas for approximately 15 min. A solution of sodium dithionite (2.20 g, 12.6 mmol) in LOW (50 mL) was added to the solution, and the reaction mixture was stirred for 4 h at room temperature. Chloroform (50 mL) was added to the solution and the organic phase was extracted and then dried over anhydrous Na₂SO₄. After removing the solvent, the residue was purified by open column chromatography using silica gel and subsequent elution with a mixture of chloroform: acetone (10:1) to produce compound **6**

as a purple solid (0.20 g, 49.6%). ¹H NMR (CDCl₃): δ 1.16 (3H, t, CH₃), 1.28 (3H, t, CH₃), 2.94 (2H, m, CH), 3.19 (1H, t, CH), 3.35 (1H, q, CH), 3.64 (2H, m, CH), 3.77 (1H, m, CH), 4.09 [4H, m, CH₂], 4.29 (2H, q, CH), 4.63 (1H, d, NH), FAB-MS (M+H)⁺: m/z 524, 526, Found: 524, 526.

Synthesis of Ethylene Dicycysteine Oxorhenium(V) (^{185/187}Re-EC) (7). A solution of 1 N NaOH (1.5 mL) was added to the solution of compound **6** (250 mg, 0.48 mmol) in ethanol (2 mL). After standing for 4 h at room temperature, ethanol was evaporated in vacuo. The pH of the solution was adjusted to 3.5 with 10% citric acid, and then compound **7** was obtained by precipitation (0.14 g, 61.8%). ¹H NMR (D₂O): δ 2.91 (1H, t, CH), 3.04 (1H, m, CH), 3.15 (2H, m, CH₂), 3.49 (m, 3H, CH₃), 3.83 (2H, q, CH), 4.34 (1H, d, NH), FAB-MS (M+H)⁺: m/z 468 and 470. Found: 468 and 470.

Synthesis of ^{185/187}Re-EC-[(D-Asp)₅]₂ (8). This compound was synthesized by the reaction of ^{185/187}Re-EC and [(D-Asp)(OtBu)]₅-resin, according to the procedure described above in yields of 13.3% (4.08 mg, compound **8a**) and 38.1% (7.54 mg, compound **8b**). ESI-MS: Re-EC-[(D-Asp)₅]₂ (M-H)⁻; m/z 1617 and 1619, Found: 1617 and 1619. Re-EC-(D-Asp)₅ (M-H)⁻; m/z 1042 and 1044, Found: 1042 and 1044.

Preparation of Sn-GH kit and ^{99m}Tc-GH. A freeze-dried kit containing 4 g of glucoheptonate (GH) and 1.2 mg of SnCl₂·2H₂O was prepared using Milli Q water at pH 8.5. ^{99m}Tc-GH was prepared by adding ^{99m}TcO₄⁻ solution (0.25 mL) to a GH kit (1 mg) to give the final GH concentration of 4 mg/mL.

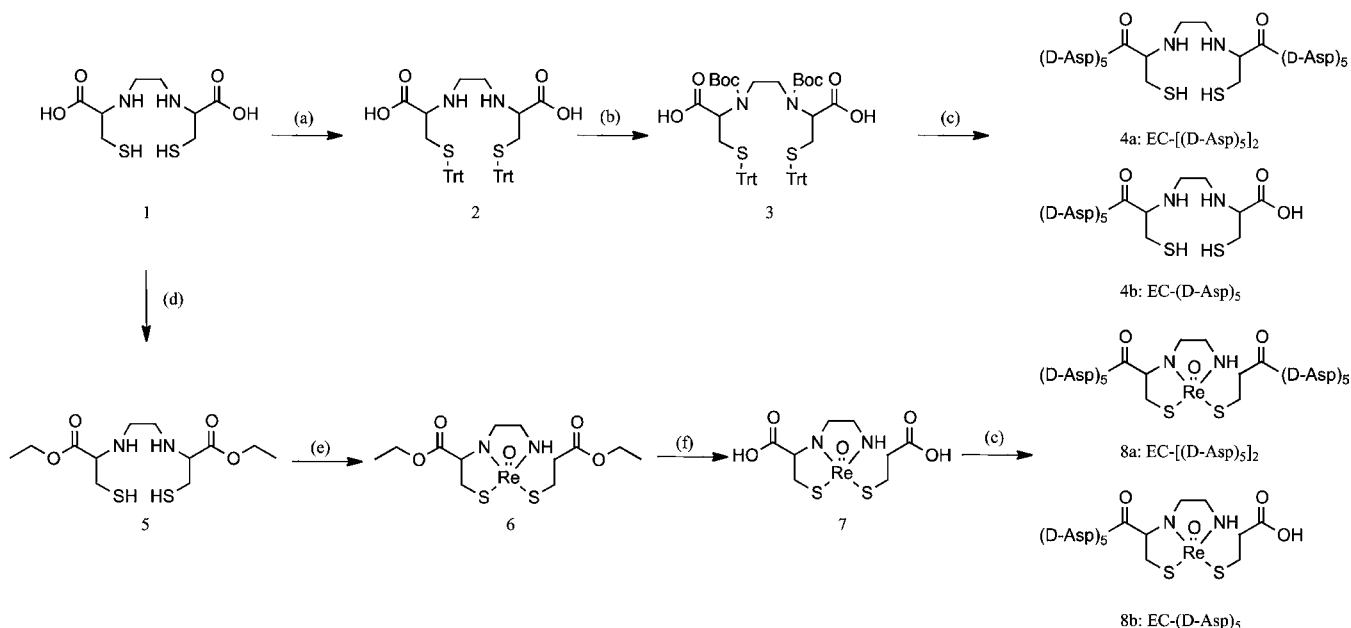
Preparation of ^{99m}Tc-EC-[(D-Asp)₅]₂ and ^{99m}Tc-EC-(D-Asp)₅. EC-[(D-Asp)₅]₂ or EC-(D-Asp)₅ (0.10 μ mol) were dissolved in 0.1 M Tris-HCl buffer (pH 9.0, 100 μ L). To the solution was added 100 μ L of the ^{99m}Tc-GH solution. The solution was standing at room temperature for 30 min and diluted 10-fold with saline before use. Radiochemical purity was determined by RP-HPLC and PC.

Preparation of ^{99m}Tc-MDP. ^{99m}TcO₄⁻ (1–2 mL) was added to the MDP-kit (Fujifilm RI Pharma. Co. Ltd.). The solution was maintained 10 min at room temperature and diluted 1–1000-fold with saline before use. Since ^{99m}Tc-MDP is not well-defined chemical species, but mixtures of short- and long-chain polymers, the concentration of free MDP in ^{99m}Tc-MDP is unknown. Thus, in this study, the concentration of MDP in ^{99m}Tc-MDP was expressed by dividing the amount of MDP by the volume of ^{99m}Tc-MDP solution. The final concentration of MDP in ^{99m}Tc-MDP was 0.02–2 mM. Radiochemical purity was determined by TLC and PC.

Plasma Stability. ^{99m}Tc-EC-[(D-Asp)₅]₂ or ^{99m}Tc-EC-(D-Asp)₅ (20 μ L) were mixed with 380 μ L of freshly prepared murine plasma at 37 $^{\circ}\text{C}$. After 10 min and 1 h, aliquots of samples (1 μ L) were drawn, diluted with saline (ca. 100 μ L), and the radioactivity was analyzed by RP-HPLC after filtration with a 10 kDa cutoff membrane (Microcon-10, Millipore Japan, Tokyo).

Plasma Protein Binding. ^{99m}Tc-EC-[(D-Asp)₅]₂ or ^{99m}Tc-EC-(D-Asp)₅ (20 μ L) were mixed with 380 μ L of freshly prepared murine plasma at 37 $^{\circ}\text{C}$. Ten min after the incubation, aliquots of samples (1 μ L) were drawn, and the radioactivity was analyzed by TLC.

Comparison of Molecular Size. The apparent molecular sizes of the ^{99m}Tc-labeled compounds were estimated by comparing their permeability through a 10-kDa and 30-kDa cutoff regenerated cellulose membrane (Amicon Ultra, NMWL 10000 and 30000, Millipore). Each ^{99m}Tc-labeled compound (3

Scheme 1. Synthetic Procedures of EC-[(D-Asp)₅]₂, EC-(D-Asp)₅, Re-EC-[(D-Asp)₅]₂, and Re-EC-(D-Asp)₅^a


^a(a) Trt-OH, TFA; (b) (Boc)₂O; (c) [D-Asp(OtBu)]₅-resin, HOBT, DIPCL, TFA; (d) EtOH, HCl; (e) NH₄ReO₄, Na₂S₂O₄; (f) 1 N NaOH/EtOH.

mL) in 0.1 M citric buffer (pH 2.5) or 0.1 M phosphate buffer (pH 7.4 or pH 9.0) were applied onto the Amicon Ultra filter. After centrifuging (780g, 5 min for NMWL 30000 or 10 min for NMWL 10000), aliquots (100 μ L) of samples in applied or filtrated solution were drawn, and the radioactivity in each fraction was measured by gamma counter ($n = 3$).

Hydroxyapatite (HA) Binding. HA beads (Bio Gel, Bio Rad, Hercules, CA) were suspended in Tris-buffered saline (TBS; 150 mM NaCl, 50 mM Tris-HCl, pH 7.4) at 10 mg/mL. To the HA suspension (100 μ L) was added 50 μ L of TBS and 50 μ L of ^{99m}Tc-EC (50 μ M), ^{99m}Tc-EC-[(D-Asp)₅]₂ (50 μ M), ^{99m}Tc-EC-(D-Asp)₅ (50 μ M), or ^{99m}Tc-MDP (21.3 μ M), and the mixture was gently agitated for 1 h at room temperature. The mixture was then centrifuged (10,000g, 5 min) and the supernatant and the precipitate were separated before the radioactivity counts in the supernatant fraction (100 μ L) were determined with an auto well gamma counter. Control studies were performed under similar conditions in the absence of HA. HA binding (%) was calculated as follows:

$$\text{HA binding(\%)} = 100 - \left[\frac{\text{(radioactivity of the supernatant of each sample)}}{\text{(radioactivity of the supernatant in the respective control)}} \right] \times 100$$

Biodistribution Studies. Animal studies were conducted in accordance with the institutional guidelines approved by the Chiba University Animal Care Committee. Biodistribution studies were performed by the intravenous administration of ^{99m}Tc-EC-(D-Asp)₅, ^{99m}Tc-EC-[(D-Asp)₅]₂ (5 μ M, 100 μ L), or ^{99m}Tc-MDP (21.3 μ M, 100 μ L) to 5-week-old male ddY mice.²⁸ Groups of four to five mice each were administered the respective ^{99m}Tc-labeled compound before sacrificing at 10 min, 1 h, 3 h, and 6 h postinjection by decapitation. Tissues of interest were removed, weighed, and the radioactivity counts were determined with an auto well gamma counter.

Cell Culture. The prostate carcinoma cell line AT6-1 was purchased from European Collection of Cell Cultures and cultured on plastic surface in RPMI 1640 medium (Sigma-Aldrich, Tokyo) supplemented with 10% fetal bovine serum and 250 nM dexamethasone at 37 °C under 5% CO₂ atmosphere.

Osteogenic Bone Tumor Bearing Rat. Osteogenic bone tumor bearing rats were made according to the procedure as reported previously with slightly modification as follows.²⁹ Four-week-old male Sprague-Dawley rats (150–180 g) were used. Animals were anesthetized with pentobarbital and the distal femoral medullar cavity was injected with 50 μ L of either alginate solution (1.2%) alone (right femur) or alginate solution containing 6×10^6 tumor cells (left femur). The cavities were sealed using bone wax and the wounds were closed with surgical suture. At 8 weeks after operation, these rats were used for in vivo imaging studies.

In Vivo Imaging. ^{99m}Tc-EC-[(D-Asp)₅]₂ (17–24 MBq, 250 μ L, 250 μ M) or ^{99m}Tc-MDP (20–23 MBq, 250 μ L, 2 mM) were administrated intravenously. After 1 h injection of each ^{99m}Tc-labeled compound, rats were anesthetized by isoflurane (1.5%, 1 L/min). SPECT imaging and X-ray CT imaging were performed by a SPECT/CT system (FX-3200, gamma Medica Inc., CA) equipped with five pinholes (0.5 mm) collimator, and 30-min data acquisition was performed. The osteogenic bone tumor to normal bone region ratios were determined by drawing regions of interest (ROI) on SPECT images (counts/pixel). The ROI of osteogenic bone tumor region was drawn manually around the edge of the tumor region activity by visual inspection. The ROI of normal bone region was drawn at the corresponding site of the contralateral tibia. ($n = 3$).

Statistical Analysis. Data are expressed as the means \pm SD where appropriate. Results were statistically analyzed using the unpaired Student's *t* test. Differences were considered statistically significant when *p* was <0.05.

RESULTS

Preparation of $^{99m}\text{Tc}/^{185/187}\text{Re}$ -Labeled Compounds. $^{99m}\text{Tc-EC}[(\text{D-Asp})_5]_2$, $^{99m}\text{Tc-EC}(\text{D-Asp})_5$, $^{185/187}\text{Re-EC}[(\text{D-Asp})_5]_2$, and $^{185/187}\text{Re-EC}(\text{D-Asp})_5$ were synthesized according to the procedure outlined in Scheme 1. $^{99m}\text{Tc-EC}[(\text{D-Asp})_5]_2$ showed a single radioactivity peak on RP-HPLC at retention time similar to that of $^{185/187}\text{Re-EC}[(\text{D-Asp})_5]_2$ (Figure 2). On

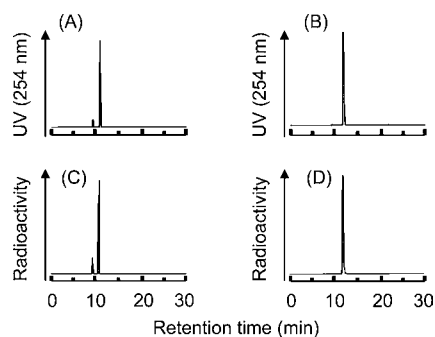


Figure 2. RP-HPLC elution profiles of $^{185/187}\text{Re-EC}(\text{D-Asp})_5$ (A) and $^{185/187}\text{Re-EC}[(\text{D-Asp})_5]_2$ (B) as determined by UV (254 nm) trace and $^{99m}\text{Tc-EC}(\text{D-Asp})_5$ (C) and $^{99m}\text{Tc-EC}[(\text{D-Asp})_5]_2$ (D) as determined by radioactivity trace. Radioactivity trace of $^{99m}\text{Tc-EC}(\text{D-Asp})_5$ and $^{99m}\text{Tc-EC}[(\text{D-Asp})_5]_2$ showed retention times identical to those of nonradioactive Re-counterparts.

the other hand, $^{99m}\text{Tc-EC}(\text{D-Asp})_5$ showed two radioactivity peaks on RP-HPLC at retention times similar to those of $^{185/187}\text{Re-EC}(\text{D-Asp})_5$ (Figure 2). ESI-MS of the two peaks showed a m/z of 1042 and 1044 (M-H^-), indicating that $^{99m}\text{Tc-EC}(\text{D-Asp})_5$ and $^{185/187}\text{Re-EC}(\text{D-Asp})_5$ eluted as well-separated isomers under the condition. $^{99m}\text{Tc-EC}[(\text{D-Asp})_5]_2$ and $^{99m}\text{Tc-EC}(\text{D-Asp})_5$ were obtained with radiochemical purities over 97%, respectively. $^{99m}\text{TcO}_2$ was not observed.

HA Binding. The HA binding rates of $^{99m}\text{Tc-EC}[(\text{D-Asp})_5]_2$, $^{99m}\text{Tc-EC}(\text{D-Asp})_5$, and $^{99m}\text{Tc-MDP}$ were over 90% at HA amount of 1.0 mg (Figure 3). With a decrease in HA amount, the binding rates of the three ^{99m}Tc -labeled compounds decreased. However, $^{99m}\text{Tc-EC}[(\text{D-Asp})_5]_2$ exhibited HA binding rates similar to and significant higher than did $^{99m}\text{Tc-MDP}$ and $^{99m}\text{Tc-EC}(\text{D-Asp})_5$ at HA amount from 0.01 mg to 0.1 mg. The HA binding of $^{99m}\text{Tc-EC}$ was not observed.

Plasma Stability and Plasma Protein Binding. After 1 h incubation of both $^{99m}\text{Tc-EC}[(\text{D-Asp})_5]_2$ and $^{99m}\text{Tc-EC}(\text{D-Asp})_5$ in murine plasma, over 94% of the two ^{99m}Tc -labeled

compounds remained intact. The protein-bound fractions of $^{99m}\text{Tc-EC}[(\text{D-Asp})_5]_2$ and $^{99m}\text{Tc-EC}(\text{D-Asp})_5$ were $0.23 \pm 0.05\%$ and $0.14 \pm 0.03\%$, respectively, when incubated in murine plasma for 10 min.

Molecular Size. Figure 4 shows the permeability of $^{99m}\text{Tc-EC}[(\text{D-Asp})_5]_2$, $^{99m}\text{Tc-EC}(\text{D-Asp})_5$ and $^{99m}\text{Tc-MDP}$ through a

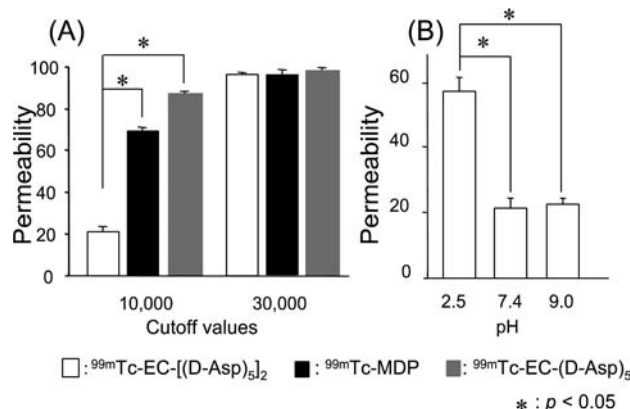


Figure 4. Permeability of ^{99m}Tc -labeled compounds through 10 kDa (left) or 30 kDa (right) cutoff membrane (A). The permeability of $^{99m}\text{Tc-EC}[(\text{D-Asp})_5]_2$ through 10 kDa cutoff membrane in solutions of different pH (pH 2.5, pH 7.4 and pH 9.0) (B). Significances were determined by unpaired Student's t test (*: $p < 0.05$ compared to $^{99m}\text{Tc-EC}[(\text{D-Asp})_5]_2$ (A) and the permeability of $^{99m}\text{Tc-EC}[(\text{D-Asp})_5]_2$ at pH 2.5 (B)).

regenerated cellulose membrane. While all ^{99m}Tc -labeled probes passed through a 30 kDa cutoff membrane, $^{99m}\text{Tc-EC}[(\text{D-Asp})_5]_2$ registered significantly lower permeability (20%) than did $^{99m}\text{Tc-MDP}$ (68%) and $^{99m}\text{Tc-EC}(\text{D-Asp})_5$ (88.5%) through a 10 kDa cutoff membrane. The permeability of $^{99m}\text{Tc-EC}[(\text{D-Asp})_5]_2$ significantly increased when the permeability was determined under acidic condition (Figure 4B).

Biodistribution Study. The biodistribution of radioactivity after administration of $^{99m}\text{Tc-EC}[(\text{D-Asp})_5]_2$, $^{99m}\text{Tc-EC}(\text{D-Asp})_5$, or $^{99m}\text{Tc-MDP}$ to mice is summarized in Table 1. $^{99m}\text{Tc-MDP}$ showed the highest radioactivity levels in the bone, followed by $^{99m}\text{Tc-EC}[(\text{D-Asp})_5]_2$ and $^{99m}\text{Tc-EC}(\text{D-Asp})_5$. In osteogenic bone tumor bearing rat, the SUV of $^{99m}\text{Tc-EC}[(\text{D-Asp})_5]_2$ in the tumor and normal region was 0.11 ± 0.04 and 0.05 ± 0.01 , respectively (Figure 5). On the other hand, the SUV of $^{99m}\text{Tc-MDP}$ in the tumor and normal region was 0.16 ± 0.08 and 0.14 ± 0.06 , respectively (Figure 5). As a result, the osteogenic bone tumor to normal bone ratios of $^{99m}\text{Tc-EC}[(\text{D-Asp})_5]_2$

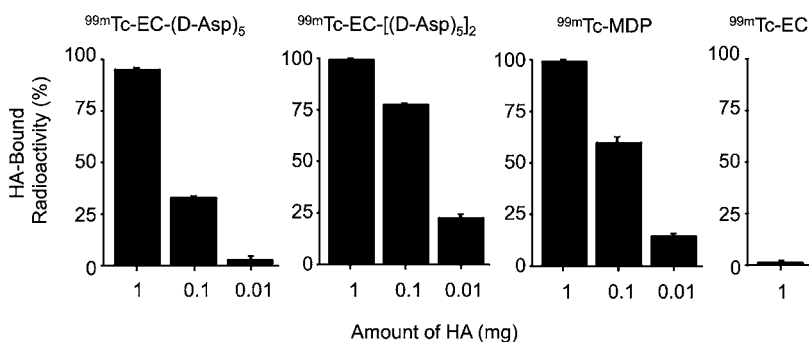


Figure 3. Binding of HA to $^{99m}\text{Tc-EC}(\text{D-Asp})_5$, $^{99m}\text{Tc-EC}[(\text{D-Asp})_5]_2$, $^{99m}\text{Tc-MDP}$, and $^{99m}\text{Tc-EC}$. Data are expressed as mean SD for 3 experiments.

Table 1. Biodistribution of Radioactivity in Mice after Injection of $^{99m}\text{Tc-EC}[(\text{D-Asp})_5]_2$, $^{99m}\text{Tc-EC}(\text{D-Asp})_5$, and $^{99m}\text{Tc-MDP}^a$

	time after injection			
	10 min	1 h	3 h	6 h
$^{99m}\text{Tc-EC}[(\text{D-Asp})_5]_2$				
Blood	2.42 (0.36)	0.11 (0.01)	0.03 (0.01)	0.02 (0.00)
Bone	18.08 (1.89)	27.33 (0.87)	19.10 (3.03)	15.60 (2.68)
Liver	0.62 (0.13)	0.15 (0.01)	0.16 (0.07)	0.13 (0.03)
Kidney	9.17 (3.01)	2.77 (0.62)	2.26 (0.34)	1.28 (0.20)
Stomach ^b	0.26 (0.05)	0.04 (0.01)	0.03 (0.02)	0.14 (0.22)
$^{99m}\text{Tc-EC}(\text{D-Asp})_5$				
Blood	2.83 (0.17)	0.22 (0.05)*	0.13 (0.03)*	0.07 (0.02)*
Bone	11.08 (0.85)*	9.57 (1.44)*	8.06 (1.06)*	6.80 (0.80)*
Liver	0.72 (0.05)	0.17 (0.02)	0.20 (0.03)*	0.18 (0.02)
Kidney	10.58 (3.81)	5.05 (1.56)*	5.00 (1.01)*	4.21 (0.89)*
Stomach ^b	0.28 (0.03)	0.04 (0.16)	0.08 (0.02)*	0.12 (0.11)
$^{99m}\text{Tc-MDP}$				
Blood	2.21 (0.27)	0.18 (0.01)*	0.11 (0.01)*	0.06 (0.01)
Bone	28.40 (3.47)*	33.41 (1.87)*	25.70 (1.59)*	26.82 (1.44)*
Liver	0.60 (0.06)	0.22 (0.06)	0.13 (0.03)	0.13 (0.01)
Kidney	7.16 (1.90)	1.61 (0.22)*	1.03 (0.11)*	0.92 (0.23)
Stomach ^b	0.55 (0.09)*	0.77 (0.20)*	0.40 (0.09)*	0.27 (0.08)

^aTissue radioactivity is expressed as % ID/g for each group ($n = 4-5$); results are expressed as mean (SD). Significances determined by unpaired student's *t*-test; (*) $p < 0.05$ compared to $^{99m}\text{Tc-EC}[(\text{D-Asp})_5]_2$. ^bExpressed as %ID.

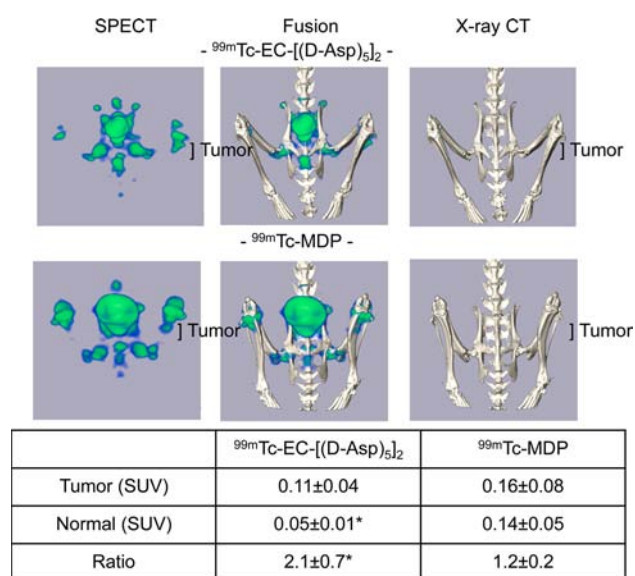


Figure 5. $^{99m}\text{Tc-EC}[(\text{D-Asp})_5]_2$ (17–24 MBq) or $^{99m}\text{Tc-MDP}$ (20–23 MBq) were administrated intravenously to osteogenic tumor bearing rats. After 1 h injection of each ^{99m}Tc -labeled compound, rats were anesthetized by isoflurane. SPECT imaging and X-ray CT imaging were performed by use of SPECT/CT system equipped with a five pinhole (0.5 mm) collimator, and 30-min data acquisition was performed. The osteogenic tumor region to normal region ratios of $^{99m}\text{Tc-EC}[(\text{D-Asp})_5]_2$ (left, ratio: 2.1) were significantly higher than those of $^{99m}\text{Tc-MDP}$ (right, ratio: 1.2). Significances were determined unpaired Student's *t* test (*: $p < 0.05$ compared to $^{99m}\text{Tc-MDP}$).

$^{99m}\text{Tc-EC}[(\text{D-Asp})_5]_2$ and $^{99m}\text{Tc-MDP}$ were 2.1 ± 0.7 and 1.2 ± 0.2 , respectively (Figure 5).

DISCUSSION

We hypothesized that specific accumulation in osteogenic bone tumor region could be achieved by a ^{99m}Tc -labeled probe that possesses strong HA binding affinity and an appropriate

molecular size when considering different vascular permeability between normal and osteogenic bone tumor regions. Our prior study showed that radiolabeled PAMAM dendrimer derivatives with molecular sizes larger than 5 nm exhibited significant accumulation in the liver or kidney with relatively slow elimination rates from the blood.³⁰ Meanwhile, it is known that vascular permeability of molecules significantly changes when the molecular weight changes from hundreds to thousands.^{31–33} Prior studies also showed that oligo-aspartic acid selectively accumulated in the bone,²² and that dendrimer derivatives with terminal ionization groups lead to a more expanded overall conformation.³⁴ These findings encouraged us to utilize penta-D-Asp as both a HA binding motif and a molecular size modifier, and $^{99m}\text{Tc-EC}[(\text{D-Asp})_5]_2$ was designed and synthesized as a prototype ^{99m}Tc -labeled probe to achieve selective accumulation in osteogenic bone tumor region.

The comparative RP-HPLC profiles of $^{99m}\text{Tc-EC}[(\text{D-Asp})_5]_2$ and $^{99m}\text{Tc-EC}(\text{D-Asp})_5$ and their $^{185/187}\text{Re}$ counterparts supported that both ^{99m}Tc -labeled compounds and their rhenium counterparts would possess similar chemical structures (Figure 2). The high plasma stability of the two ^{99m}Tc -labeled compounds also supported their chemical structures when recalling high in vivo stability of $^{99m}\text{Tc-EC}$ derivatives reported so far.^{9,35} However, while $^{99m}\text{Tc-EC}[(\text{D-Asp})_5]_2$ provided a single ^{99m}Tc complex, $^{99m}\text{Tc-EC}(\text{D-Asp})_5$ generated two ^{99m}Tc complexes due to formation of anti and syn isomers, as have been observed with many ^{99m}Tc complexes of N_2S_2 type ligands.³⁶ In HA binding experiments, $^{99m}\text{Tc-EC}[(\text{D-Asp})_5]_2$ exhibited higher HA binding affinity than did $^{99m}\text{Tc-EC}(\text{D-Asp})_5$ (Figure 3), which reinforced that the HA binding affinity of oligo-D-Asp compounds increased with an increase in Asp number.²² This study also indicated that the HA binding of oligo-D-Asp increased when the two (D-Asp)₅ motifs were connected via a $^{99m}\text{Tc-EC}$ chelate. The HA binding of $^{99m}\text{Tc-EC}[(\text{D-Asp})_5]_2$ was similar to those of $^{99m}\text{Tc-MDP}$ and $^{99m}\text{Tc}/^{186}\text{Re}$ -labeled chelated bisphosphonate derivatives.^{37,10}

To compare apparent molecular size of $^{99m}\text{Tc-EC}[(\text{D-Asp})_5]_2$, $^{99m}\text{Tc-EC}(\text{D-Asp})_5$, and $^{99m}\text{Tc-MDP}$, the membrane permeability of the three compounds was estimated (Figure 4). Since all the tested compounds were almost quantitatively excluded from a 30 kDa cutoff membrane, all compounds should possess apparent molecular weight less than 30 kDa. These results also indicated that adsorption of all compounds onto the membrane was negligible. The permeability through a 10 kDa cutoff membrane, however, exhibited significant difference among the three ^{99m}Tc -labeled compounds, and suggested that $^{99m}\text{Tc-EC}[(\text{D-Asp})_5]_2$ was the least permeable through normal blood vessels, due to its apparent greatest molecular size of the three. The significant increase in the membrane permeable fractions of $^{99m}\text{Tc-EC}[(\text{D-Asp})_5]_2$ at pH lower than the dissociation pH of the β -carboxylic acid of Asp supported the present chemical design that the repulsion of the ionization form of each carboxylic acid in $^{99m}\text{Tc-EC}[(\text{D-Asp})_5]_2$ would be responsible for the apparent high molecular size (Figure 4B). The gathered in vitro studies indicated that $^{99m}\text{Tc-EC}[(\text{D-Asp})_5]_2$ is a single compound that possesses high plasma stability and strong HA binding ability with molecular size higher than those of $^{99m}\text{Tc-EC}(\text{D-Asp})_5$ and $^{99m}\text{Tc-MDP}$.

In biodistribution studies, $^{99m}\text{Tc-EC}[(\text{D-Asp})_5]_2$ showed higher uptake in murine bone than did $^{99m}\text{Tc-EC}(\text{D-Asp})_5$, which reflected higher HA binding ability of $^{99m}\text{Tc-EC}[(\text{D-Asp})_5]_2$. This also reinforced that the affinities of oligo-aspartic acid to bone increased with increasing peptide chain length and the peptides consisting of over six residues were selectively distributed to the bone.²² On the other hand, the normal bone accumulation of $^{99m}\text{Tc-EC}[(\text{D-Asp})_5]_2$ was significantly lower than that of $^{99m}\text{Tc-MDP}$, despite their similar HA binding abilities (Table 1 and Figure 3). The bone accumulation of $^{99m}\text{Tc-EC}[(\text{D-Asp})_5]_2$ was also significantly lower than those of [^{186}Re]CpTR-, $^{99m}\text{Tc-MAG}_3$ -, and $^{99m}\text{Tc-HYNIC}$ -conjugated bisphosphonate derivatives, although all the compounds exhibited similar HA binding under similar experimental conditions.^{37,10} The accumulation of $^{99m}\text{Tc-EC}[(\text{D-Asp})_5]_2$ in normal rat bone was also lower than that of $^{99m}\text{Tc-MDP}$, which was well visualized when comparing the radioactivity levels of the two ^{99m}Tc -labeled compounds in bone joints (Figure 5). However, $^{99m}\text{Tc-EC}[(\text{D-Asp})_5]_2$ exhibited accumulation in the bone tumor region similar to that of $^{99m}\text{Tc-MDP}$ (Figure 5). As a result, $^{99m}\text{Tc-EC}[(\text{D-Asp})_5]_2$ provided higher tumor-to-normal bone region ratios, which was reflected in the superior image of the bone tumor region. The findings in this study supported our working hypothesis that selective targeting to the osteogenic bone region would be achieved by a ^{99m}Tc -labeled compound with high HA binding and an appropriate molecular size that possesses different vascular permeability between normal and osteogenic bone tumor regions.

In conclusion, a mononuclear $^{99m}\text{Tc-EC}$ chelate was derivatized with two (penta-D-Asp) groups as both a HA binding motif and a molecular size modifier for selective accumulation in osteogenic tumor region. The ^{99m}Tc -labeled probe exhibited accumulation in the osteogenic tumor and normal bone region similar to and significantly lower than $^{99m}\text{Tc-MDP}$, respectively. Although further studies on optimization of the chain length of oligo-D-Asp are required, these findings indicate that the present chemical design of ^{99m}Tc -labeled probe would be applicable to develop ^{99m}Tc -labeled probes for selective visualization of osteogenic tumor region. These findings also suggest that the present chemical

design would provide a good basis for developing a new drug delivery system to deliver therapeutic radionuclides such as ^{186}Re , ^{188}Re , ^{90}Y , or ^{177}Lu and cytotoxic drugs to osteogenic tumor region.

■ ASSOCIATED CONTENT

Supporting Information

Elemental analyses data of N,N' -bis-*tert*-butoxycarbonyl- S,S' -bis-triphenylmethyl-ethylene dicysteine [$\text{EC}(\text{Boc})_2(\text{Trt})_2$] and ethylene dicysteine oxorhenium(V) ($^{185/188}\text{Re-EC}$). This material is available free of charge via the Internet at <http://pubs.acs.org>.

■ AUTHOR INFORMATION

Corresponding Author

*Tel: +81-43-226-2898, FAX: +81-43-226-2897, E-mail: tuehara@chiba-u.jp.

Notes

The authors declare no competing financial interest.

■ ACKNOWLEDGMENTS

This study was supported in part by a Grant-in-Aid for Young Scientists (B) and Special Funds for Education and Research (Development of SPECT Probes for Pharmaceutical Innovation) from the Ministry of Education, Culture, Sports, Science and Technology of Japan.

■ REFERENCES

- (1) Palma, E., Correia, J. D. G., Campello, M. P. C., and Santos, I. (2011) Bisphosphonates as radionuclide carriers for imaging or systemic therapy. *Mol. BioSyst.* 7, 2950–2966.
- (2) Mayer-Kuckuk, P., and Boskey, A. L. (2006) Molecular imaging promotes progress in orthopedic research. *Bone* 39, 965–977.
- (3) Ryan, P. J., and Fogelman, I. (1997) Bone scintigraphy in metabolic bone disease. *Semin. Nucl. Med.* 27, 291–305.
- (4) Buckley, O., O'Keefe, S., Geoghegan, T., Lyburn, I. D., Munk, P. L., Worsley, D., and Torreggiani, W. C. (2007) ^{99m}Tc bone scintigraphy superscans: a review. *Nucl. Med. Commun.* 28, 521–527.
- (5) Tanabe, S., Zodda, J. P., Libson, K., Deutsch, E., and Heineman, W. R. (1983) The biological distributions of some technetium-MDP components isolated by anion exchange high performance liquid chromatography. *Int. J. Appl. Radiat. Isot.* 34, 1585–1592.
- (6) Pinkerton, T. C., Heineman, W. R., and Deutsch, E. (1980) Separation of technetium hydroxyethylidene dihydrophosphate complexes by anion-exchange high performance liquid chromatography. *Anal. Chem.* 52, 1106–1110.
- (7) Love, C., Din, A. S., Tomas, M. B., Kalappambath, T. P., and Palestro, C. J. (2003) Radionuclide bone imaging: an illustrative review. *Radiographics* 23, 341–358.
- (8) Fogelman, I. (1982) Diphosphonate bone scanning agents—current concepts. *Eur. J. Nucl. Med.* 7, 506–509.
- (9) Verbeke, K., Rozenski, J., Cleynhens, B., Vanbilloen, H., de Groot, T., Weyns, N., Bormans, G., and Verbruggen, A. (2002) Development of a conjugate of $^{99m}\text{Tc-EC}$ with aminomethylenediphosphonate in the search for a bone tracer with fast clearance from soft tissue. *Bioconjugate Chem.* 13, 16–22.
- (10) Ogawa, K., Mukai, T., Inoue, Y., Ono, M., and Saji, H. (2006) Development of a novel ^{99m}Tc -chelate-conjugated bisphosphonate with high affinity for bone as a bone scintigraphic agent. *J. Nucl. Med.* 47, 2042–2047.
- (11) Ogawa, K., Mukai, T., Asano, D., Kawashima, H., Kinuya, S., Shiba, K., Hashimoto, K., Mori, H., and Saji, H. (2007) Therapeutic effects of a ^{186}Re -complex-conjugated bisphosphonate for the palliation of metastatic bone pain in an animal model. *J. Nucl. Med.* 48, 122–127.

- (12) Shukla, G., Tiwari, A. K., Sinha, D., Srivastava, R., Cahndra, H., and Mishra, A. K. (2009) Synthesis and assessment of ^{99m}Tc chelate-conjugated alendronate for development of specific radiopharmaceuticals. *Cancer Biother. Radiopharm.* 24, 209–214.
- (13) Ogawa, K., Mukai, T., Kawai, K., Takamura, N., Hanaoka, H., Hashimoto, K., Shiba, K., Mori, H., and Saji, H. (2009) Usefulness of competitive inhibitors of protein binding for improving the pharmacokinetics of ^{186}Re -MAG₃-conjugated bisphosphonate (^{186}Re -MAG₃-HBP), an agent for treatment of painful bone metastases. *Eur. J. Nucl. Med. Mol. Imaging* 36, 115–121.
- (14) Datta, A., Panwar, P., Chuttani, K., and Mishra, A. K. (2009) Synthesis of ^{99m}Tc -DOTMP and its preclinical evaluation as a multidentate imaging agent for skeletal metastases. *Cancer Biother. Radiopharm.* 24, 123–128.
- (15) Palma, E., Correia, J. D. G., Oliveira, B. L., Gano, L., Santos, I. C., and Santos, I. (2011) $^{99m}\text{Tc}(\text{CO})_3$ -labeled pamidronate and alendronate for bone imaging. *Dalton Trans.* 40, 2787–2796.
- (16) Ogawa, K., Mukai, T., Arano, Y., Otaka, A., Ueda, M., Uehara, T., Magata, Y., Hashimoto, K., and Saji, H. (2006) Rhenium-186-monoaminemonoamidedithiol-conjugated bisphosphonate derivatives for bone pain palliation. *Nucl. Med. Biol.* 33, 513–520.
- (17) Hansen-Algenstaedt, N., Joscheck, C., Wolfram, L., Schaefer, C., Muller, I., Bottcher, A., Deuretzbacher, G., Wiesner, L., Leunig, M., Algenstaedt, P., and Ruther, W. (2006) Sequential changes in vessel formation and micro-vascular function during bone repair. *Acta Orthop. Scand.* 77, 429–439.
- (18) Yuan, F., Dellian, M., Fukumura, D., Leunig, M., Berk, D. A., Torchilin, V. P., and Jain, R. K. (1995) Vascular permeability in a human tumor xenograft: molecular size dependence and cutoff size. *Cancer Res.* 55, 3752–3756.
- (19) Hansen-Algenstaedt, N., Joscheck, C., Schaefer, C., Lamszus, K., Wolfram, L., Biermann, T., Algenstaedt, P., Brockmann, M. A., Heintz, C., Fiedler, W., and Ruther, W. (2005) Long-term observation reveals time-course-dependent characteristics of tumour vascularisation. *Eur. J. Cancer* 41, 1073–1085.
- (20) Kasugai, S., Fujisawa, R., Waki, Y., Miyamoto, K., and Ohya, K. (2000) Selective drug delivery system to bone: small peptide Asp₆ conjugation. *J. Bone Miner. Res.* 15, 936–943.
- (21) Wang, D., Miller, S., Sima, M., Kopeckova, P., and Kopecek, J. (2003) Synthesis and evaluation of water-soluble polymeric bone-targeted drug delivery systems. *Bioconjugate Chem.* 14, 853–859.
- (22) Sekido, T., Sakura, N., Higashi, Y., Miya, K., Nitta, Y., Nomura, M., Sawanishi, H., Morito, K., Masamune, Y., Kasugai, S., Yokogawa, K., and Miyamoto, K. (2001) Novel drug delivery system to bone using acidic oligopeptide: pharmacokinetic characteristics and pharmacological potential. *J. Drug Targeting* 9, 111–121.
- (23) Uehara, T., Ishii, D., Uemura, T., Suzuki, H., Kanei, T., Takagi, K., Takama, M., Murakami, M., Akizawa, H., and Arano, Y. (2010) Gamma-Glutamyl PAMAM dendrimer as versatile precursor for dendrimer-based targeting devices. *Bioconjugate Chem.* 21, 175–181.
- (24) Blondeau, P., Berse, C., and Grabel, D. (1967) Dimerization of an intermediate during the sodium in liquid ammonia reduction of L-thiazoline-4-carboxylic acid. *Can. J. Chem.*, 49–52.
- (25) Arano, Y., Akizawa, H., Uezono, T., Akaji, K., Ono, M., Funakoshi, S., Koizumi, M., Yokoyama, A., Kiso, Y., and Saji, H. (1997) Conventional and high-yield synthesis of DTPA-conjugated peptides: application of a monoreactive DTPA to DTPA-D-Phe¹-octreotide synthesis. *Bioconjugate Chem.* 8, 442–446.
- (26) Kaiser, E., Colese, R. L., Bossinger, C. D., and Cook, P. I. (1970) Color test for detection of free terminal amino groups in the solid-phase synthesis of peptides. *Anal. Biochem.* 34, 595–598.
- (27) Green, J. M., Jones, R., Harrison, R. D., Edwards, D. S., and Glajch, J. L. (1993) Liquid chromatographic separation of radiopharmaceutical ligand enantiomers. *J. Chromatogr.* 635, 203–209.
- (28) Imai, S., Morimoto, J., Tsubura, T., Esaki, K., Michalides, R., Holms, R. S., Delimling, O., and Higlers, J. (1986) Genetic marker patterns and endogeneous mammary tumor virus genes in inbred mouse strains in japan. *Jikken Dobutsu* 35, 263–273.
- (29) Lamoureux, F., Ory, B., Battaglia, S., Pilet, P., Heymann, M. F., Gouin, F., Duteille, F., Heymann, D., and Redini, F. (2008) Relevance of a new rat model of osteoblastic metastases from prostate carcinoma for preclinical studies using zoledronic acid. *Int. J. Cancer* 122, 751–760.
- (30) Uehara, T., Ishii, D., Uemura, T., Suzuki, H., Kanei, T., Takagi, K., Takama, M., Murakami, M., Akizawa, H., and Arano, Y. (2010) gamma-Glutamyl PAMAM dendrimer as versatile precursor for dendrimer-based targeting devices. *Bioconjugate Chem.* 21, 175–181.
- (31) Pappenheimer, J. R. (1953) Passage of molecules through capillary walls. *Physiol. Rev.* 33, 387–423.
- (32) Schmittmann, G., and Rohr, U. D. (2000) Comparison of the permeability surface product (PS) of the blood capillary wall in skeletal muscle tissue of various species and in vitro porous membranes using hydrophilic drugs. *J. Pharm. Sci.* 89, 115–127.
- (33) Curry, F. E., Huxley, V. H., and Adamson, R. H. (1983) Permeability of single capillaries to intermediate-sized colored solutes. *Am. J. Physiol.* 245, H495–505.
- (34) Chen, W., Tomalia, D. A., and Thomas, J. L. (2000) Unusual pH-dependent polarity changes in PAMAM dendrimers: evidence for pH-responsive conformational changes. *Macromolecules* 33, 9169–9172.
- (35) Yang, D. J., Kim, C. G., Schechter, N. R., Azhdarinia, A., Yu, D. F., Oh, C. S., Bryant, J. L., Won, J. J., Kim, E. E., and Podoloff, D. A. (2003) Imaging with ^{99m}Tc ECDG targeted at the multifunctional glucose transport system: feasibility study with rodents. *Radiology* 226, 465–473.
- (36) Luyt, L. G., Jenkins, H. A., and Hunter, D. H. (1999) An N₂S₂ bifunctional chelator for technetium-99m and rhenium: complexation, conjugation, and epimerization to a single isomer. *Bioconjugate Chem.* 10, 470–479.
- (37) Uehara, T., Jin, Z. L., Ogawa, K., Akizawa, H., Hashimoto, K., Nakayama, M., and Arano, Y. (2007) Assessment of ^{186}Re chelate-conjugated bisphosphonate for the development of new radiopharmaceuticals for bones. *Nucl. Med. Biol.* 34, 79–87.